# SuFExable polymers with helical structures derived from thionyl tetrafluoride

Li, Suhua; Li, Gencheng; Gao, Bing; Pujari, Sidharam P.; Chen, Xiaoyan et al

# SuFExable polymers with helical structures derived from thionyl tetrafluoride

Suhua Li [1,2 ✉], Gencheng Li[2], Bing Gao[2], Sidharam P. Pujari [3], Xiaoyan Chen[1], Hyunseok Kim [2], Feng Zhou[4], Liana M. Klivansky[5], Yi Liu [5], Hafedh Driss[6], Dong-Dong Liang[3], Jianmei Lu [4], Peng Wu [7 ✉], Han Zuilhof [3,6,8 ✉], John Moses[9 ✉] and K. Barry Sharpless [2 ✉]

Sulfur(VI) fluoride exchange (SuFEx) is a category of click chemistry that enables covalent linking of modular units through sulfur(VI) connective hubs. The efficiency of SuFEx and the stability of the resulting bonds have led to polymer chemistry applications. Now, we report the SuFEx click chemistry synthesis of several structurally diverse $SOF_4$-derived copolymers based on the polymerization of bis(iminosulfur oxydifluorides) and bis(aryl silyl ethers). This polymer class presents two key characteristics. First, the [–N=S(=O)F–O–] polymer backbone linkages are themselves SuFExable and undergo precise SuFEx-based post-modification with phenols or amines to yield branched functional polymers. Second, studies of individual polymer chains of several of these new materials indicate helical polymer structures. The robust nature of SuFEx click chemistry offers the potential for post-polymerization modification, enabling the synthesis of materials with control over composition and conformation.

The inspiration behind the invention of modular click chemistry came from an appreciation of how nature synthesizes its most essential molecules, the primary metabolites. These polynucleotides, polypeptides and polysaccharides from the union of discrete modules by carbon–heteroatom connections[1,2]. Since describing the underpinning philosophy of click chemistry, two key click reactions have emerged that enable the formation of stable connections with unparalleled efficiency. The Cu(I)-catalysed azide–alkyne cycloaddition reaction (CuAAC) was reported independently by the groups of Meldal[3] and Sharpless[4] in 2002, while Sharpless and colleagues advanced the sulfur fluoride exchange (SuFEx) reaction in 2014[5]. CuAAC has had a perspective-changing impact in many fields, not least drug discovery[6–9], bioconjugation[10,11] and materials science[12–15]. In polymer chemistry, CuAAC is predominately used for backbone functionalization rather than for polymerization[16,17].

SuFEx click chemistry[18–22] is characterized by the exchange of aryl silyl ethers or amines, often through discrete SuFExable hubs such as sulfuryl fluoride ($SO_2F_2$)[5], thionyl tetrafluoride ($SOF_4$)[23,24], ethenesulfonyl fluoride (ESF)[5,18,25] and 1-bromoethene-sulfonyl fluoride (BESF)[26–28] (Fig. 1). Dong, Gao and co-workers were among the first to recognize the potential of SuFEx for polymer synthesis. Exploiting the powerful combination of reaction efficiency and linkage stability, the researchers synthesized several $SO_2F_2$-derived polysulfate–SuFEx copolymers of bis(aryl silyl ethers) with bis(aryl fluorosulfates) in the presence of 1,8-diazabicyclo[5.4.0]undec-7-ene (DBU) or the highly efficient catalyst $(Me_2N)_3S^+[FHF]^-$ (Fig. 1b)[29,30]. Wu et al. reported the high-yielding synthesis of polysulfonate SuFEx polymers, employing a bifluoride ion-catalysed polycondensation of ESF-derived bis(alkylsulfonyl fluorides) with

bis(aryl silyl ethers) (Fig. 1b)[31]. The mild conditions enable SuFEx polymerization reactions to proceed efficiently without causing substantial increases in temperature during the reaction[29,30], delivering novel materials with fascinating properties, including hydrolytic stability, thermal stability and tensile modulus.

Encouraged by the successful applications of $SO_2F_2$ and ESF in SuFEx polymer chemistry, we have explored thionyl tetrafluoride ($SOF_4$)[23] as a new connective hub[23] for use in polymer synthesis. Unlike the $SO_2F_2$ and ESF SuFExable hubs, $SOF_4$ is a multidimensional connector that forms discrete connections via a stereogenic sulfur(VI) centre (for example, R–N=S(=O)(F)–OR′).

The unique connectivity potential of $SOF_4$ creates countless opportunities for click chemistry[23] and, in the context of polymer science, a chance to overcome the incredibly challenging goal of post-polymerization modification of the polymer spine (Fig. 1c).

In this Article, we report the synthesis of a family of helical SuFEx polymers from copolymerization of bis(aryl silyl ethers) and the $SOF_4$-derived bis(iminosulfur oxydifluorides). The powerful combination of highly efficient SuFEx reactivity and robust SuFEx-enabled post-polymerization modifications enables the synthesis of materials with rational control of composition, conformation and functionality.

## Results and discussion

**Polymer synthesis.** The bis(iminosulfur oxydifluoride) **1-1** (prepared, as previously described, from $SOF_4$[23] and 4,4′-diaminodiphenyl sulfone) and the bisphenol A bis(t-butyldimethylsilyl ether)[29,30] **2-1** were chosen as model substrates. In our earlier SuFEx work with $SOF_4$, we found that, under DBU catalysis, it is possible to exchange just one of the bis(iminosulfur oxydifluoride) S–F bonds. The products

[1]School of Chemistry, Sun Yat-Sen University, Guangzhou, People's Republic of China. [2]Department of Chemistry and The Skaggs Institute for Chemical Biology, The Scripps Research Institute, La Jolla, CA, USA. [3]Laboratory of Organic Chemistry, Wageningen University, Wageningen, Netherlands. [4]College of Chemistry, Chemical Engineering and Materials Science, Collaborative Innovation Center of Suzhou Nano Science and Technology, Soochow University, Suzhou, China. [5]The Molecular Foundry, Lawrence Berkeley National Laboratory, Berkeley, CA, USA. [6]Department of Chemical and Materials Engineering, Faculty of Engineering, King Abdulaziz University, Jeddah, Saudi Arabia. [7]Department of Molecular Medicine, The Scripps Research Institute, La Jolla, CA, USA. [8]School of Pharmaceutical Sciences and Technology, Tianjin University, Tianjin, People's Republic of China. [9]Cold Spring Harbor Laboratory, New York, NY, USA. ✉e-mail: lisuhua5@mail.sysu.edu.cn; pengwu@scripps.edu; han.zuilhof@wur.nl; moses@cshl.edu; sharpless@scripps.edu
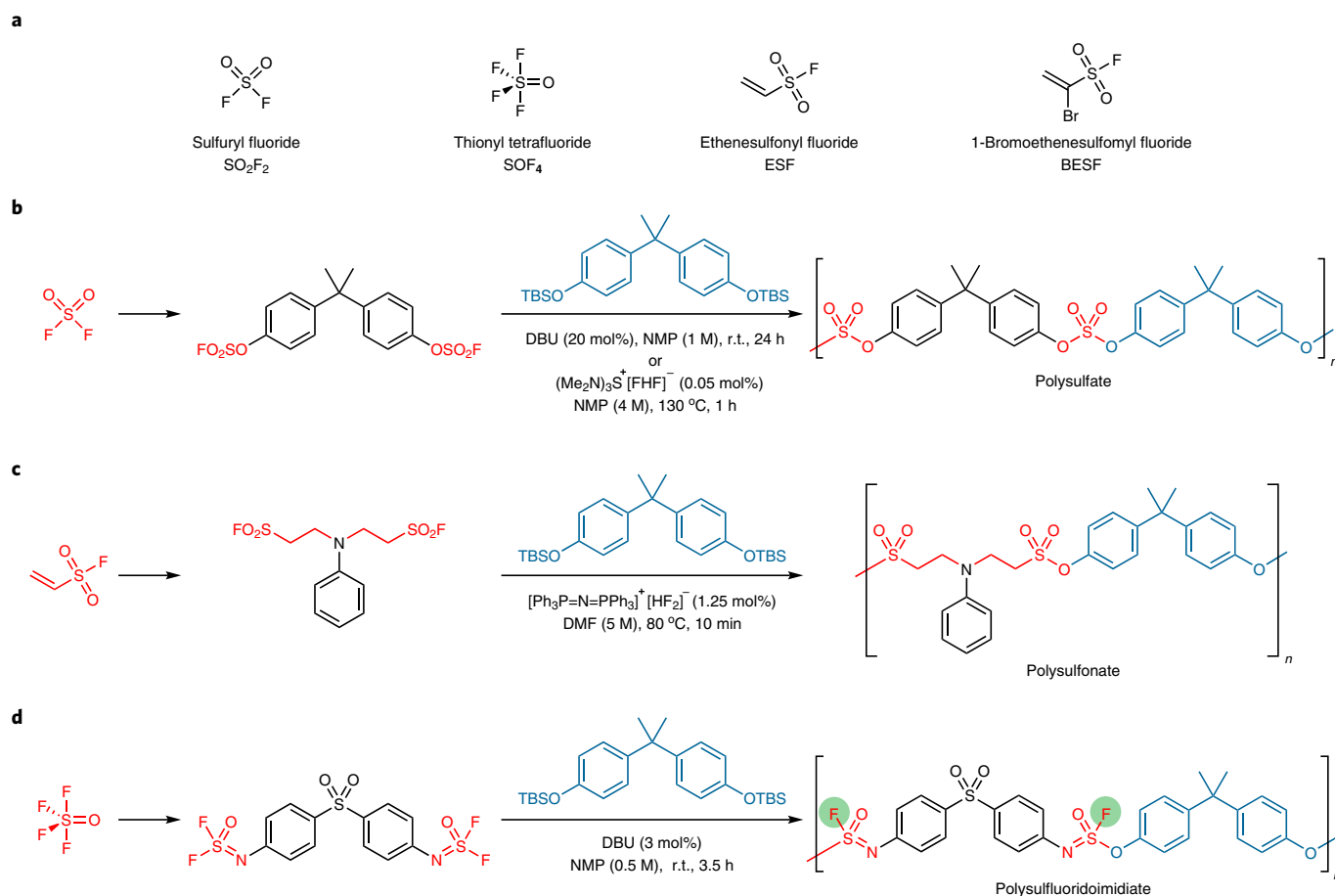
**Fig. 1 | SuFEx click chemistry for polymer synthesis. a**, Connective SuFEx hubs for creating S-centred linkages. **b**, Polysulfate materials derived from SO$_2$F$_2$. **c**, Polysulfonate materials obtained from ESF. **d**, Polysulfluoridoimidate materials derived from the multidimensional SuFEx connector SOF$_4$ (this work). Connective hubs are shown in red. Silyl ether-protected bisphenol monomers are shown in pale blue. SuFExable S–F bonds for post-polymerization backbone modification are highlighted in green.

have a single S–F bond remaining, which is less reactive due to the attenuated electrophilicity at sulfur. Nevertheless, under more forcing SuFEx conditions, this S–F bond is also exchangeable. We anticipated that using sub-stoichiometric quantities of DBU would allow the polymerization process to proceed through just one of the two available S–F bonds of each iminosulfur oxydifluoride group, thereby avoiding crosslinking and branching reactions[23].

The addition of DBU (2 mol%)[5,29] to a solution of the difluoride (1 equiv.) and silyl ether (1 equiv.) in *N*-methyl-2-pyrrolidone (NMP) at room temperature gave an observable reaction almost immediately, with the solution becoming noticeably more viscous. Stirring the reaction mixture for a further 5 min resulted in the formation of a syrupy solution accompanied by a slight increase in the reaction temperature (to ~40–50 °C). After 3.5 h of reaction time, the colourless [Ar–N=S(=O)(F)–OAr]-linked polymer **3-1** was isolated in 99% yield with a weight-averaged molecular mass ($M_w$) of 197 kDa (containing ~326 monomers and with a polydispersity index (PDI) of 1.8; Fig. 1d). (For reactions performed on a 5 mmol scale, a slight increase in catalyst loading to 3 mol% of DBU was required for efficient polymerization.)
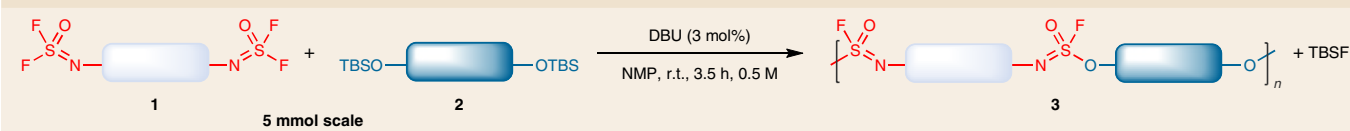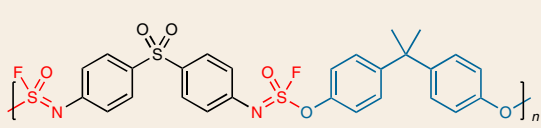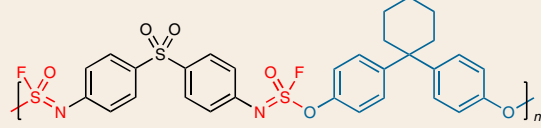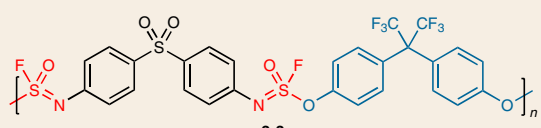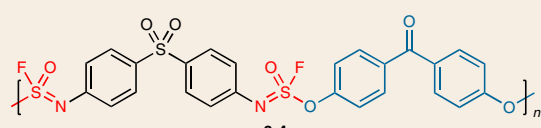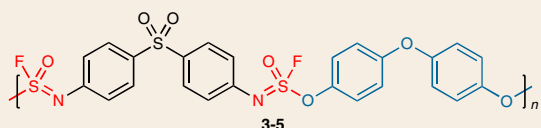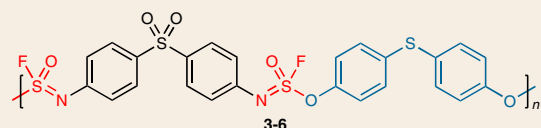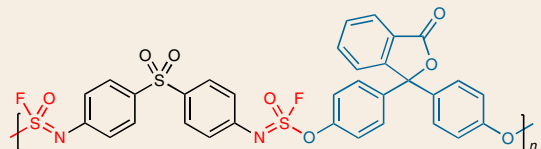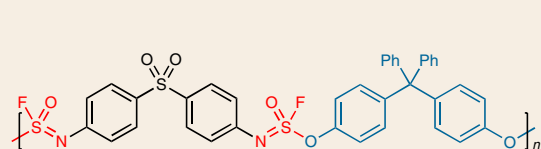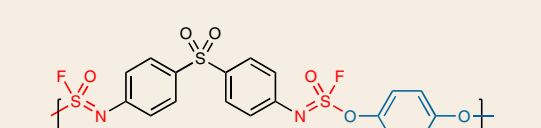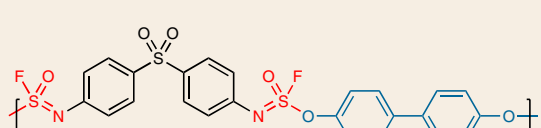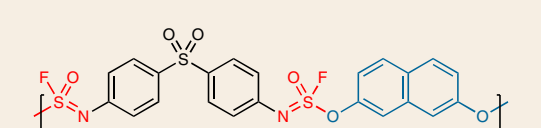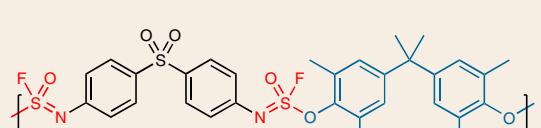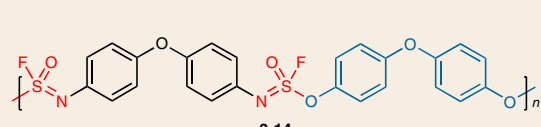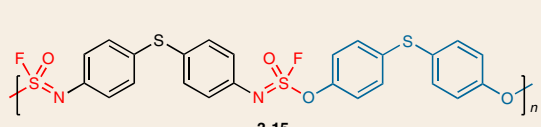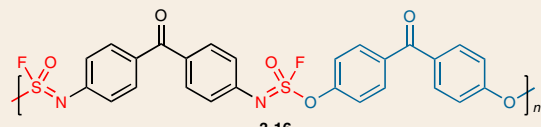
With confirmation that the SOF$_4$-derived iminosulfur oxydifluoride connectors are incorporated smoothly into the polymer spine, we next explored the potential of this SuFEx polymerization reaction to access structurally different polymers from a diverse set of building blocks. Hence, the DBU-mediated polymerization of **1-1** was examined with aryl silyl ethers comprising different functional

groups (**2-1**–**2-12**, Supplementary Information pages 10,11), giving the respective polymers **3-1**–**3-12** in excellent yields (82–99%, Table 1), with the distribution of molecular weights ranging from 36 to 295 kDa and typical PDIs of ~1.7 (values ranging from 1.4 to 2.3). Similarly, the SuFEx polymerization reaction worked equally well with a selection of bis(iminosulfur oxydifluorides) (themselves prepared from SOF$_4$ and the corresponding bis-arylamines) and several bis(aryl silyl ethers) delivering various polymers (**3-13**–**3-31**) with excellent yields. Because of the lower reactivity of benzylic substrates, both the *meta*- and *para*-bis(benzylic iminosulfur oxydifluorides) required more extended reaction times (24 h) and an increased catalyst loading of 10 mol% DBU (**3-32** and **3-33**).

Examining the collective ¹H NMR, ¹³C NMR and ¹⁹F NMR data of the polymers revealed surprisingly uncomplicated spectra, as if belonging to a small molecule (Supplementary Information pages 97–144). Considering that the connective sulfur centre is stereogenic and could result in numerous diastereoisomers in an uncontrolled polymerization event, the spectra are curiously straightforward.
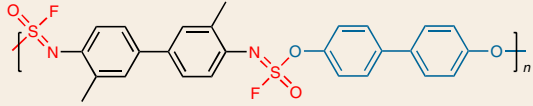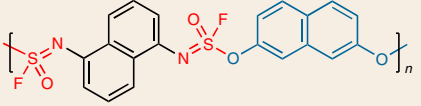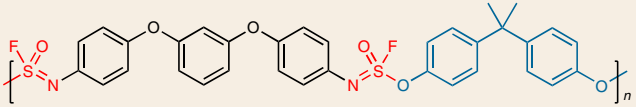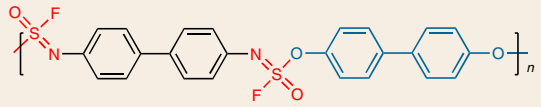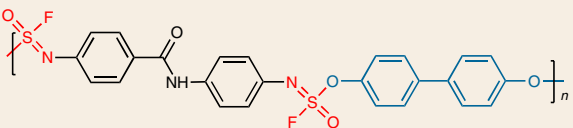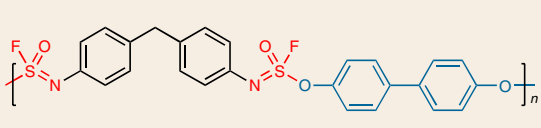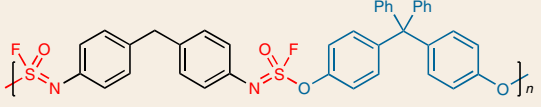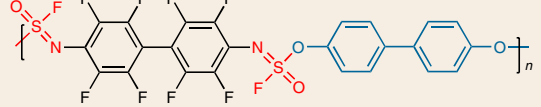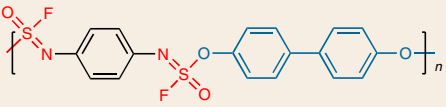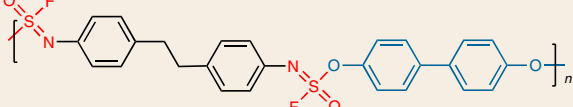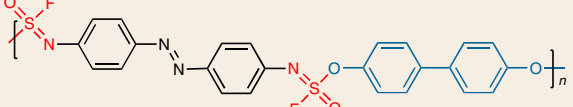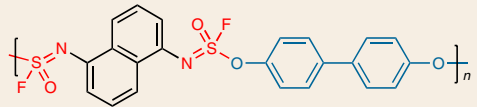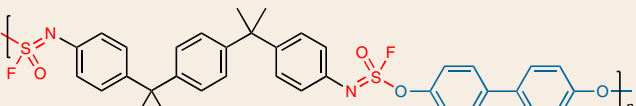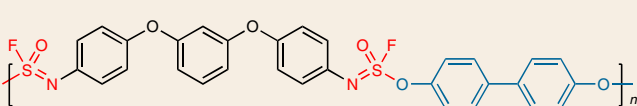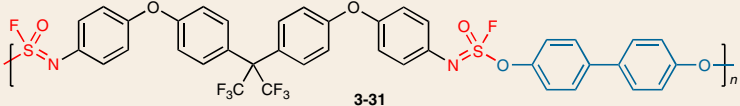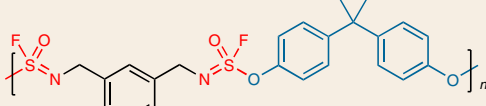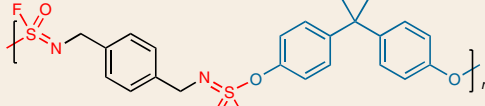
To investigate the polymerization progress in more detail, the DBU-catalysed copolymerization of **1-1** and **2-1** was monitored by sampling and quenching 20-μl aliquots of the reaction mixture every 10 s. The transformation data were calculated based on the ratio of the ¹⁹F signal integral of the remaining –N=SOF$_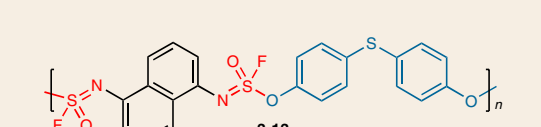2$ to the initial –N=SOF$_2$ before adding DBU. The NMR data (Supplementary Information pages 160–170) revealed that the monomer conversion was completed within 200 s (Fig. 2). The relative ratios of the ¹⁹F

## Table 1 | Synthesis of SOF₄-derived copolymers by the DBU-catalysed SuFEx polymerization of bis(iminosulfur oxydifluoride) and bis(silyl ether) monomers



**3-1**
18.0 g, 99% (30 mmol scale, 2 mol% DBU)
$M_w$ 197 kDa, PDI 1.8

**3-2**
95%, $M_w$ 57 kDa, PDI 1.6

**3-3**
93%, $M_w$ 149 kDa, PDI 1.9

**3-4**
95%, $M_w$ 112 kDa, PDI 2.1

**3-5**
89%, $M_w$ 105 kDa, PDI 1.6

**3-6**
94%, $M_w$ 235 kDa, PDI 3.0

**3-7**
93%, $M_w$ 295 kDa, PDI 2.3

**3-8**
91%, $M_w$ 87 kDa, PDI 1.7

**3-9**
92%, $M_w$ 94 kDa, PDI 1.8

**3-10**
98%, $M_w$ 176 kDa, PDI 1.8

**3-11**
95%, $M_w$ 237 kDa, PDI 2.2

**3-12**
82%, $M_w$ 36 kDa, PDI 1.4

**3-13**
97%, $M_w$ 79 kDa, PDI 2.0

**3-14**
97%, $M_w$ 107 kDa, PDI 1.7

**3-15**
93%, $M_w$ 97 kDa, PDI 2.0

**3-16**
98%, $M_w$ 53 kDa, PDI 1.7

(Continued)

**Table 1 | Synthesis of SOF$_4$-derived copolymers by the DBU-catalysed SuFEx polymerization of bis(iminosulfur oxydifluoride) and bis(silyl ether) monomers (Continued)**

**3-17**
96%, $M_w$ 57 kDa, PDI 1.5

**3-18**
96%, $M_w$ 53 kDa, PDI 1.9

**3-19**
95%, $M_w$ 63 kDa, PDI 1.6

**3-20**
93%, $M_w$ 131 kDa, PDI 1.7

**3-21**
98%, $M_w$ 110 kDa, PDI 1.8

**3-22**
99%, $M_w$ 116 kDa, PDI 1.7

**3-23**
95%, $M_w$ 44 kDa, PDI 2.2

**3-24**
99%, $M_w$ 63 kDa, PDI 1.8

**3-25**
98%, $M_w$ 124 kDa, PDI 1.7

**3-26**
98%, $M_w$ 107 kDa, PDI 1.8

**3-27**
99%, $M_w$ 118 kDa, PDI 1.7

**3-28**
98%, $M_w$ 184 kDa, PDI 1.8

**3-29**
98%, $M_w$ 89 kDa, PDI 1.7

**3-30**
99%, $M_w$ 188 kDa, PDI 1.7

**3-31**
99%, $M_w$ 157 kDa, PDI 1.8

**3-32**
95%, $M_w$ 156 kDa, PDI 1.8
(10 mol% DBU, 24 h)

**3-33**
94%, $M_w$ 103 kDa, PDI 1.7
(10 mol% DBU, 24 h)

Reaction conditions: For **3-1**: bis(iminosulfur oxydifluoride) (12.49 g, 30 mmol), bisphenol A *tert*-butyldimethylsilyl ether (BPA-TBS; 13.70 g, 30 mmol) and DBU (91.3 mg, 0.6 mmol) were reacted in 40 ml of NMP (3.5 h, room temperature (r.t.)). For **3-32** and **3-33**: bis(iminosulfur oxydifluoride) (5 mmol), bis(silyl ether) (5 mmol) and DBU (0.50 mmol) were reacted in 10 ml of NMP (24 h, r.t.). For others: bis(iminosulfur oxydifluoride) (5 mmol), bis(silyl ether) (5 mmol) and DBU (0.15 mmol) were reacted in 10 ml of NMP (3.5 h, r.t.).
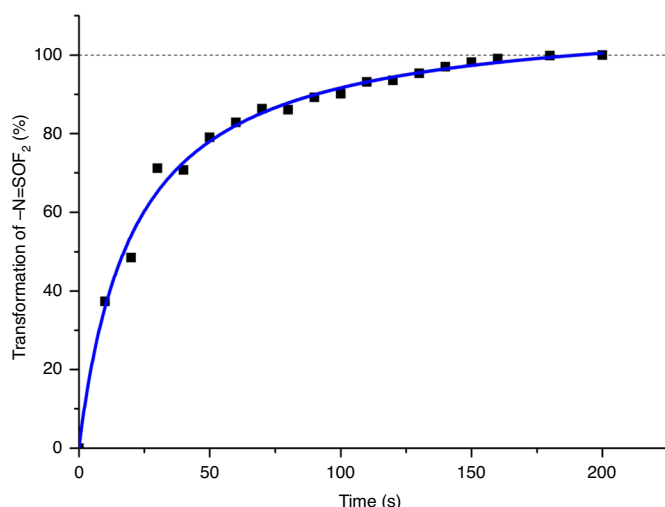
**Fig. 2 | Kinetic profile of the polymerization of 1-1 (1 mmol) and 2-1 (1 mmol) (0.5 M in NMP, 3 mol% DBU).** The monomer conversion was completed within 200 s, indicating a very fast reaction. The transformation data were calculated based on the ratio of the $^{19}F$ signal integral of the remaining $-N{=}SOF_2$ at the indicated time compared to the integral of $-N{=}SOF_2$ before adding DBU with $^{19}F$ NMR (no-solvent mode).

signals at 48.4 ppm and 48.2 ppm in the NMR spectra show a substantial initial increase of the fluoride at the polymer chain terminals, followed by a gradual decrease as the polymerization ensues. These observations are characteristic of a step-growth polymerization mechanism[32].

**Polymer functionalization.** Post-polymerization modification (PPM) is an important technique that allows the manipulation of polymer properties through synthetic modification and derivatization[33–37]. Hence, the SuFEx modification of the remaining S(VI)–F bond of the polymeric materials is advantageous. Studies on the chemistry of $SOF_4$ derivatives have shown that 2-*tert*-butylimino-2-diethylamino-1,3-dimethylperhydro-1,3,2-diazaphosphorine (BEMP) is an effective catalyst for the SuFEx of aryl silyl ethers with the remaining S(VI)–F bond of sulfurofluoridoimidates[23]. The same is true for the $SOF_4$-derived polymers—following the reaction of polymer **3-1** with *tert*-butyldimethyl(4-(1,2,2-triphenylvinyl) phenoxy)silane (**4**) and BEMP (10 mol%), the backbone-modified polymer **5** was isolated in 95% yield (Fig. 3a). Unlike the precursor polymer **3-1**, the derivative **5** displays a strong aggregation-induced emission (AIE) effect[38], dramatically enhancing photoluminescence efficiency as the water content increases from 0% to 99%. This observation is important, because AIE fluorophores have applications in many fields, including energy, optoelectronics and the life sciences, thereby presenting an important opportunity for $SOF_4$–SuFEx polymers (Fig. 3b). (For fluorescence spectra of polymer **3-1** and 4-(1,2,2-triphenylvinyl)phenol, see Supplementary Information pages 51–52.)

Additionally, the SuFEx derivatization of polymer **3-1** with the *tert*-butyl(3-ethynylphenoxy) dimethylsilane (**6**) delivers the alkyne-functionalized polymer **7** in excellent yield (Fig. 3c). The remarkable efficiency of the reaction is confirmed by the degree of substitution of at least 93% based on the ratio of methyl versus terminal alkynyl protons in the $^{1}H$ NMR results (Supplementary Information page 146). (The observed ratio would yield 93%, but it was noted that the one proton in terminal alkynes sometimes showed as slightly less than 1.00 in the $^{1}H$ NMR results.) The alkyne unit's surgical installation enables further click chemistry functionalization through CuAAC, thereby offering a unique modular

platform for creating novel functional polymers. This feature was demonstrated through further derivatization of polymer **7** with the azidothymidine (AZT) **8** under ligand-accelerated CuAAC conditions[39,40] to give the triazole-linked nucleoside polymer **9** in 96% yield. Analysis of the $^{1}H$ NMR spectrum revealed that, as far as is observable from the absence of any remaining terminal alkyne protons, all pendant alkyne groups of the parent polymer had been consumed (Supplementary Information page 147).

The reaction of the remaining S–F bonds of SuFEx polymer **3-1** was also feasible with secondary amines such as pyrrolidine (**10**) and 4-ethynylpiperidine (**11**), conveniently yielding branched polymers **12** and **13** (Fig. 3d), or with ferrocene moieties in **14** to yield polymer **15** (Fig. 3e).

**Polymer structure.** The uncomplicated $^{1}H$ NMR, $^{13}C$ NMR and $^{19}F$ NMR spectra of all the new SuFEx polymers inspired us to explore further the three-dimensional (3D) structures of these new materials. Because of the tetrahedral sulfur core of the $\sim$N=S(=O)F–O$\sim$ linkage, we anticipated that the $SOF_4$-based polymers might also display 3D features beyond random coiling, as observed for a variety of helical polymers[41,42]. We therefore assessed three representative SuFEx polymers: first **3-23**, and subsequently **3-9** and **5**, by atomic force microscopy (AFM, tapping mode), molecular mechanics studies, scanning Auger microscopy, high-resolution scanning electron microscopy (SEM) and transmission electron microscopy (TEM) measurements.

We first built a 32-mer atomistic model of the polymer **3-23**, and the structure thereof was optimized with a generically applicable force field for organic materials (polymer consistent force field, PCFF)[43] without any constraints. This model yielded a helical structure with a diameter of $4.9 \pm 0.4$ nm and pitch of 7.0 nm (Fig. 4a,b). Experimental studies of individual surface-deposited polymer chains followed.

Polymer **3-23** was dissolved in dichloromethane, and a few droplets of the solution were dispensed onto an atomically flat, hexadecyne-coated Si(111) surface[44], after which the solvent was allowed to evaporate at room temperature. Next, AFM topography images of **3-23** were obtained as deposited on these Si(111) surfaces, displaying many individual polymer wires (Fig. 4c–g). These individual polymer chains revealed a near-constant height of $4.2 \pm 0.7$ nm (inset in Fig. 4c; measurements were taken at 370 points on multiple polymer chains, like those in Fig. 4d, on the surface; Supplementary Fig. 9). This height surpasses the size of any moiety present in the polymer chain of **3-23**, but correlates very well to the theoretical prediction of the diameter of a helix formed by individual polymer chains. More detailed information on the polymer structure can be obtained from Fig. 4e, which depicts the corresponding amplitude signal map, revealing periodicity in the polymeric structures. To rule out effects of the substrate and scanning parameters on the observed periodicity, we compared the cross-sectional profiles of the polymer along the main axis of symmetry (vertical purple line, Fig. 4e) with a profile line along the same direction on the substrate (vertical yellow line, Fig. 4e). The amplitude cross-section on the polymer showed a clear periodic signal that is not present on the substrate (Fig. 4f). Fast Fourier transform (FFT) on the cross-sectional profile of the polymer was used to evaluate the polymer periodicity quantitatively (Fig. 4g). The experiment showed a dominant frequency of ~7 nm, in agreement with the polymer's calculated structure. As expected, a similar operation on the profile acquired on the substrate did not show any notable periodicity, thus excluding scanning artefacts or substrate influence.

To corroborate the polymer height obtained by AFM, we next performed high-resolution SEM analysis to determine the width of individual polymer chains, revealing a figure of $4.8 \pm 0.5$ nm (measured at 50 points on multiple polymer chains on the surface;
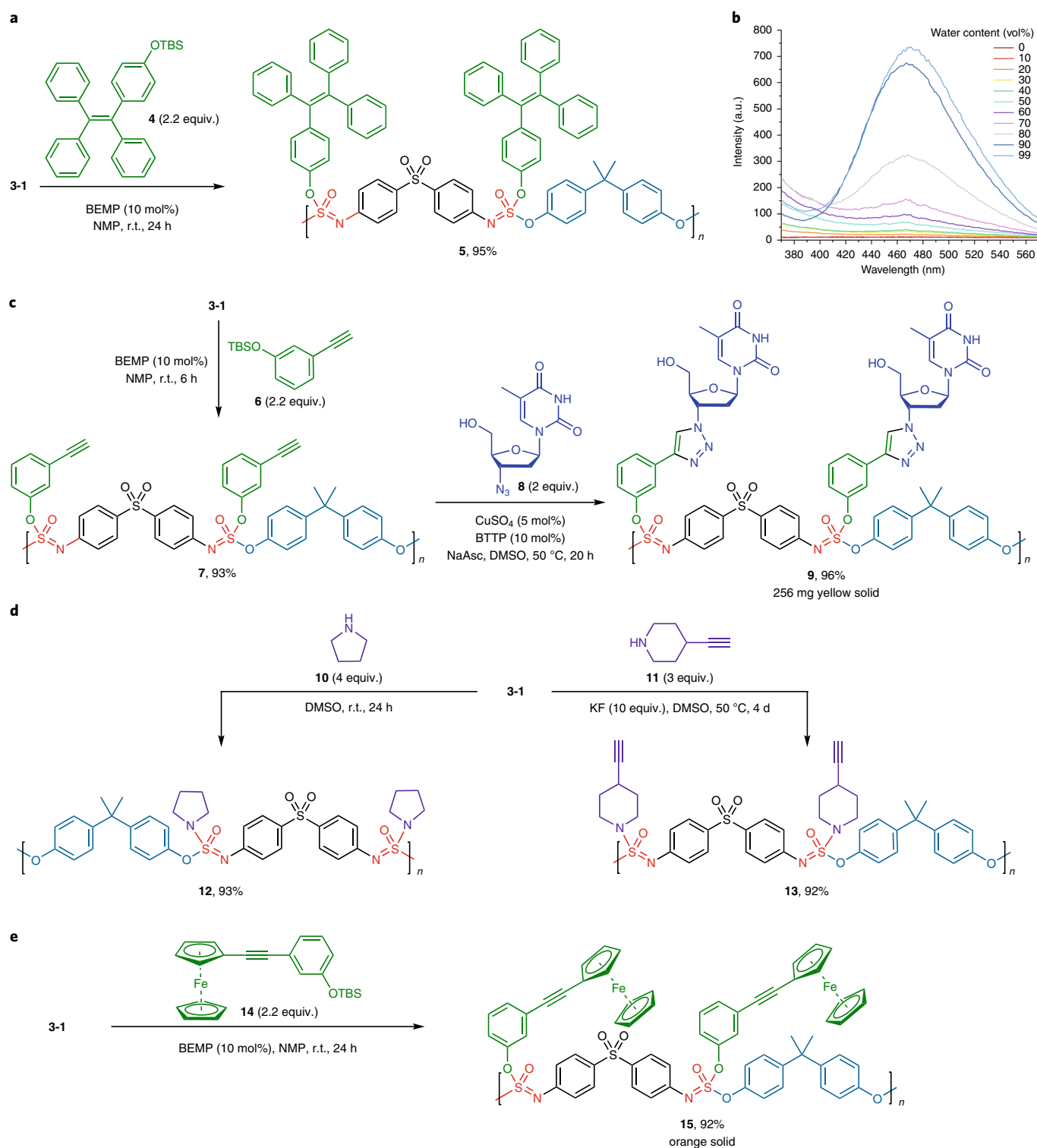
**Fig. 3 | Post-polymerization modification of polymer 3-1 using sequential SuFEx and CuAAC click chemistry. a**, SuFEx synthesis of triphenylvinyl phenoxy-branched polymer **5**. **b**, Fluorescence spectra of **5** (5 μM of the repeat unit) in THF/H₂O (vol/vol=100:0 to ~1:99), indicating a strong AIE effect. **c**, Stepwise synthesis of alkyne-functionalized polymer **7** by SuFEx (the new moiety is shown in green) and subsequent CuAAC synthesis of polymer **9** with an azide-bearing AZT derivative (shown in dark blue). **d**, Post-polymerization SuFEx modification of **3-1** with secondary amines (shown in purple). **e**, Introduction of the ferrocene unit (shown in green) to the polymer chain. All yields are the weight of polymer recovery compared with the 100% substituted polymer's theoretical weight.

Fig. 4h). The height and width agree very well with one another and the hypothesized helical character of the polymer wires (**3-23**). To confirm that the observed wires did indeed correspond to the SuFEx polymer, instead of some unidentified fibrous contamination, we performed scanning Auger microscopy (on a hexadecanethiol-modified Au surface). As can be seen in Fig. 4i, the
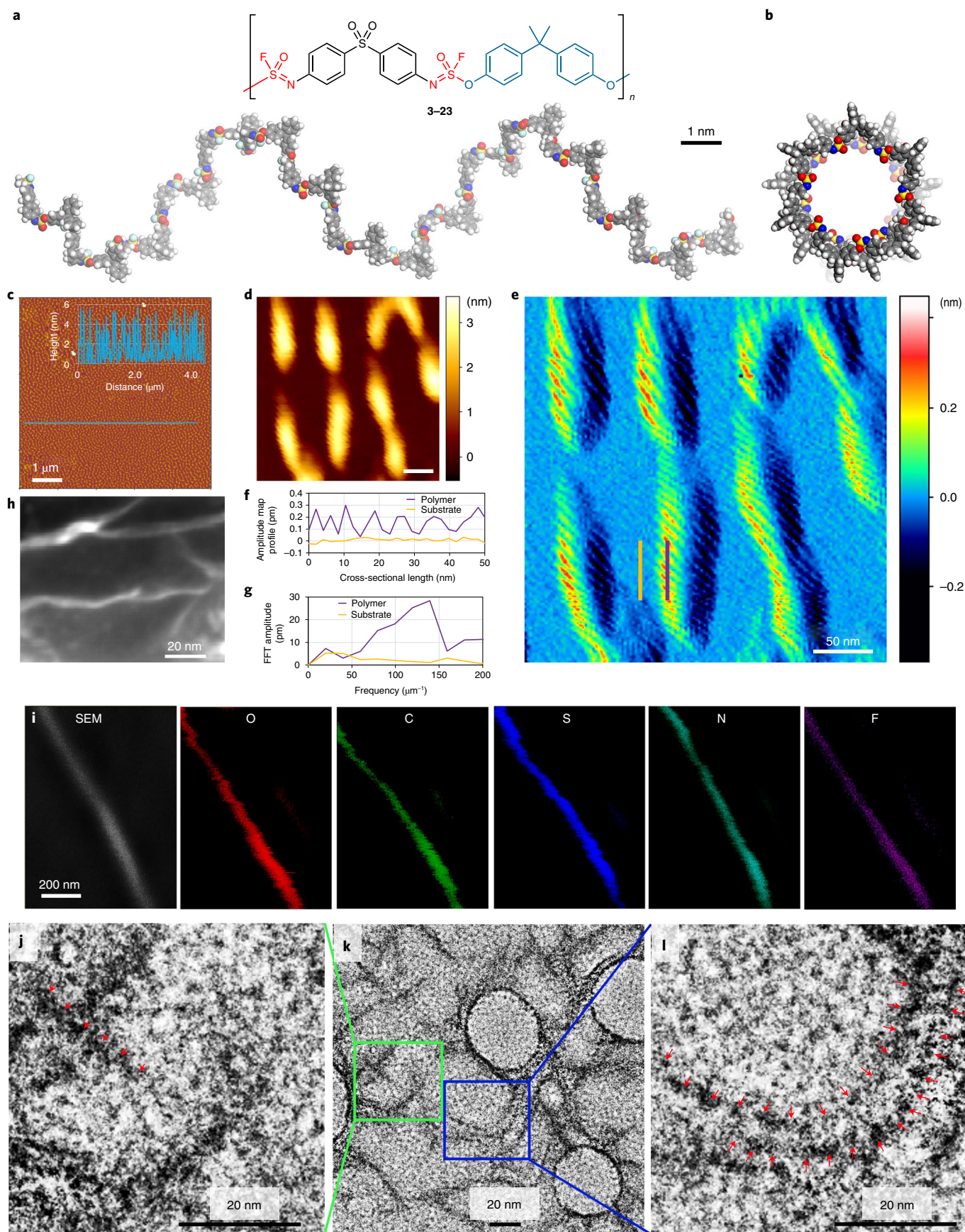
**Fig. 4 | The multidimensional connectivity of the S(VI) hubs: detailed structure studies. a,b**, PCFF-optimized structure of **3-23** in side (**a**) and top (**b**) views. Colour code of atoms: C, grey; O, red; N, blue; F, cyan; S, yellow; H, white. **c**, AFM height image ($5 \times 5\,\mu m^2$), with inset topographic height profile, showing the structural organization and periodicity of the helical polymer. **d,e**, Zoomed-in topographic image (scale bar, 50 nm) (**d**) and amplitude map (**e**) of polymer **3-23** on hexadecyne-coated Si(111) surfaces. **f,g**, Cross-sections were taken over a polymer chain (vertical purple line in **e**) and over the substrate (parallel vertical yellow line in **e**), giving cross-sectional amplitude profiles acquired on the polymer (purple) and substrate (yellow) (**f**) and fast Fourier transforms of the cross-sectional amplitude profiles on the polymer (purple) and substrate (yellow) (**g**) to extract the dominant frequencies in the signal. **h**, High-resolution SEM image of **3-23** deposited on a TEM grid. **i**, SEM image of polymer **3-23** coated on a hexadecanethiol-modified gold surface, and Auger electron spectroscopy (AES) images on the same surface for the elements O, C, S, N and F. **j–l**, High-resolution TEM image of polymer **3-23** (**k**) and zoomed-in images (**j,l**) of the areas outlined in **k** (red marks have been added as a guide to the eye to determine pitch).

wire-like structures comprise the elements expected to be present in the polymer chain, namely O, C, S, N and F, thus corroborating that the SuFEx polymer wires with functional ~N=S(=O)F–O~ moiety were indeed being observed. Finally, high-resolution TEM measurements allowed zooming in on the structure. TEM measurements (Fig. 4k) at 30 points revealed a width of $4.5 \pm 0.6$ nm for individual polymer chains, in agreement with both SEM and modelling data, thereby strongly indicating a helical structure. The zoomed-in TEM data in Fig. 4j,l then revealed a repeating structure. The red arrows in these figures are placed at points of increased intensity, which occur at highly regular intervals, as expected for a single helical polymer. This regularity is observable for individual polymer chains (Fig. 4j) and chains adjacent to each other (Fig. 4l). Analogous to the polymer structure optimized in vacuo that yields a pitch of 7.0 nm and the AFM data that yield a pitch of ~7 nm, the high-resolution TEM image yields a polymer pitch of ~$4.6 \pm 0.6$ nm (at 31 points). We tentatively attribute these differences to the attractive polymer–surface interactions and sample-to-sample variations. Such helical structures are consistent with the NMR data because random configurations would lead to broad NMR peaks, contrasting with observation.

Molecular modelling studies on 20 of the polymers from Fig. 2 predict that all form helical structures, although, for most polymers, the helical structure only displays a diameter of <1.5 nm, which would be hard to detect by AFM. We surmised that the size of the groups would strongly affect the diameter of the polymer chain. To this end, we investigated, in detail, the structure of **5** (as a polymer with a bulky substituent) and **3-9** (as a representative polymer with relatively small groups). Indeed, both **5** and **3-9** display helical structures in the modelling, with diameters of $5.7 \pm 0.4$ nm and $2 \pm 1$ nm, respectively. These values correlate very well with the AFM-measured heights of $6.9 \pm 1.1$ nm and $2.1 \pm 0.2$ nm, respectively, as well as the TEM-observed widths of $5.5 \pm 0.3$ nm and $2.3 \pm 0.4$ nm, respectively (Supplementary Figs. 15 and 12). The latter is in the range observed for double-stranded DNA helices ($2.3 \pm 0.2$ nm)[45]. Finally, large substituents do not always yield high diameters. For example, the ferrocene-linked polymer **15** was synthesized to allow a direct correlation between AFM heights in TEM-based widths, but displayed an AFM-based height of only $1.1 \pm 0.2$ nm (Supplementary Fig. 17), which itself was too small to be used in the TEM-based studies.

To understand the helical structure of these simulated polymers, the stereogenic nature of the –N=S(=O)F–O– linker must be considered. For molecular modelling studies, a 32-mer model of polymer **3-23** was constructed (Supplementary Table 1). This was achieved by copying repeat units of an enantiomerically pure monomer (in this case the *R* configuration at the stereogenic sulfur centre), by first making the dimer and then doubling four more times to obtain the 32-mer model. The helical structures obtained after geometry optimization correlate well with the experimental observations.

These observations warrant further comment. First, helicity is not exclusive to homochiral polymer models. Upon inverting one or more configurations in the chain comprising 64 putative homochiral

sulfur atoms, the helicity is retained. Also, if the *S* configuration is built into the model polymer at regular intervals (for example, $R_7 S R_7 S R_7 S R_7 S R_7 S R_7 S R_7 S$), the calculated results again predict the formation of a helical polymer, albeit with a slightly different diameter and pitch. However, with a large and fully randomized variation of *R* and *S* configurations, no helicity was predicted by the molecular modelling. The modelling data collectively indicate robustness in the helical shape that corresponds to a thermodynamic minimum (Supplementary Table 1). Second, optical activity in the polymer product would not be expected in the absence of chiral induction, and circular dichroism measurements confirm this view. Third, the observed polymer helicity suggests a degree of self-organization to give the thermodynamically preferred tertiary structures. These structures would inevitably require the SuFEx bond-forming reactions to be reversible to flip the configuration at a given sulfur centre. To investigate this, we treated the enantiomerically pure model substrate (**R**)-(−)-**16** ($[\alpha]^{20}D = -9.33$ ($c = 1.00$, CHCl$_3$)>99% e.e.; the absolute configuration was determined by anomalous dispersion method of X-ray diffraction, Supplementary Information page 39) with DBU in NMP. Significant racemization was observed after 16 h at room temperature (Fig. 5b)[46]. However, although racemization does not occur quickly for this particular model substrate, it may indeed for a polymer with an energetic preference for forming a helix.

A reaction mixture comprising **16** (0.07 M in CD$_3$CN) and DBU (0.1 M) was monitored by $^1$H NMR at room temperature, revealing a degree of hydrolysis after 22 h (Supplementary Information page 42). However, the optically pure sulfurimidate (−)-**17** (98% e.e.) is stable to racemization in both 0.1 M DBU and BEMP (0.1 M) at room temperature in CD$_3$CN (Supplementary Information pages 47–49). The reaction of (*S*)-(+)-**16** ($[\alpha]^{20}D = +6.31$ ($c = 1.00$, CHCl$_3$)) with PhOTBS in the presence of 20 mol% of BEMP gave optically pure sulfurimidate (−)-**17**, further demonstrating the stability of sulfurimidate, as well as the complete memory or inversion of chirality in this SuFEx reaction (Fig. 5a). The racemization of (**R**)-(−)-**16** is thought to occur by DBU-mediated reversible formation of the S(VI) cation. Polymer **3-1** (0.028 M repeating unit in DMF-$d_7$) and DBU (0.1 M) were observed by $^1$H NMR to undergo significant hydrolysis after 11 h (Supplementary Information page 43), indicating a greater propensity for racemization than the corresponding (**R**)-(−)-**16**.

Finally, the used collective spectroscopic techniques (AFM, SEM, AES and TEM) lead us to conclude that the polymers arise without significant branching. This observation is consistent with the established reactivity trend of SOF$_4$ derivatives[23]. For example, when monomer **1-1** was reacted to completion with 4 equiv. of aryl silyl ether **2-13** for 10 min, the ratio of products **18** to **19** was over 100:1 (Fig. 5c). The observed chemoselective preference during polymerization explains the preferential formation of the linear (unbranched) polymer.

## Conclusions

In summary, we have described a new class of modular SuFEx copolymers linked through SOF$_4$-derived [–N=S(=O)(F)–O-] hubs and
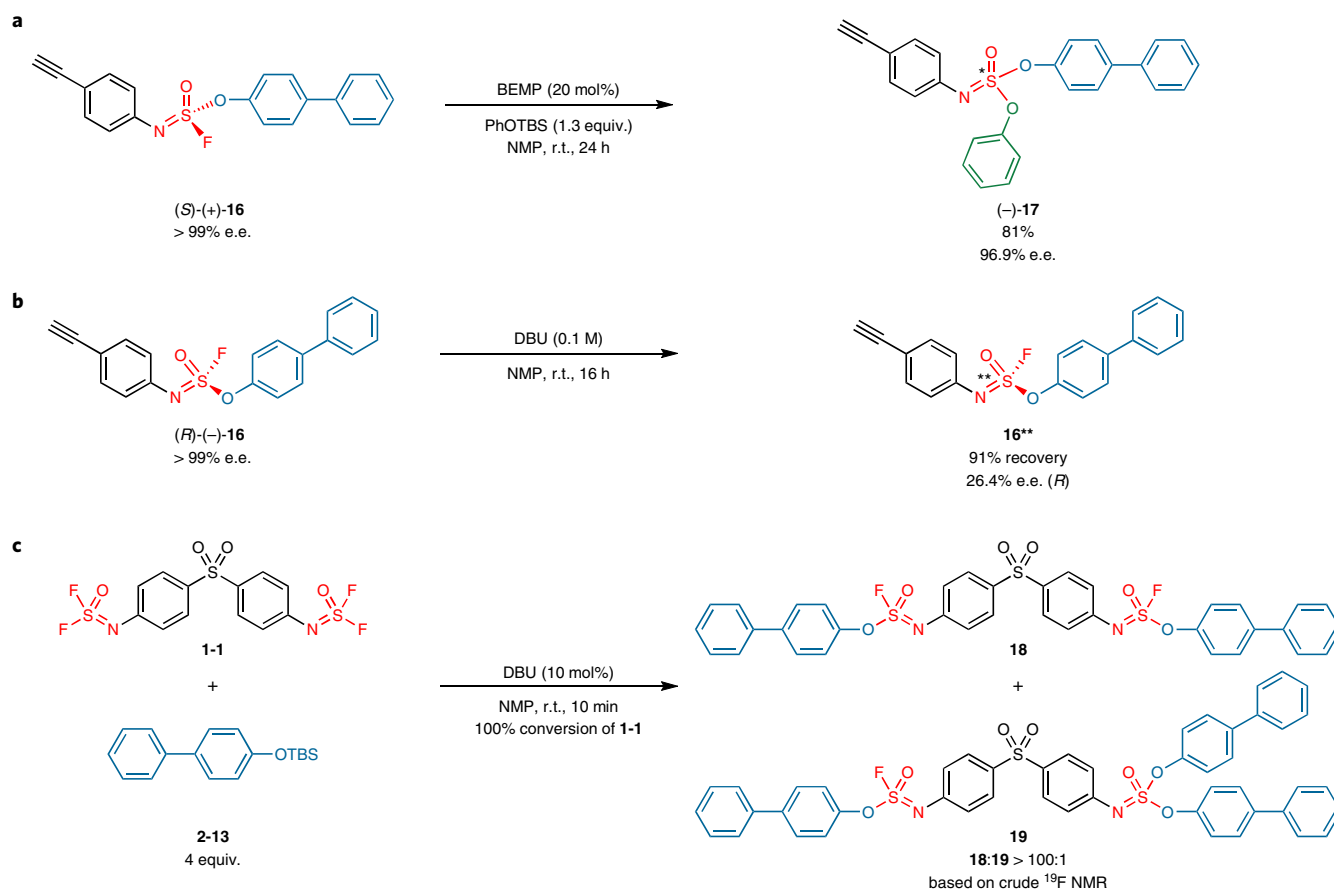
**Fig. 5 | Substitution of S–F bond of optically pure sulfurofluoridoimidate in the presence of BEMP, racemization experiment for sulfurofluoridoimidate in the presence of DBU and reactive selectivity of iminosulfur oxydifluoride with aryl silyl ether. a**, The reaction of (S)-(+)-**16** ([α]²⁰D = +6.31 (c = 1.00, CHCl₃)) with PhOTBS in the presence of 20 mol% of BEMP gave optically pure sulfurimidate (−)-**17** (96.9% e.e.), and the absolute configuration of (−)-**17** is not determined. **b**, Considerable racemization of **(R)-(−)-16** ([α]²⁰D = −9.33 (c = 1.00, CHCl₃)) appeared after 16 h in the presence of DBU (0.1 M, NMP). **c**, The selectivity between the first and secondary fluoride of iminosulfur oxydifluoride **1-1** is over 100:1, even in a large excess of an aryl silyl ether.

bisphenol monomers. These polymers were prepared with high efficiency from the corresponding bis(iminosulfur oxydifluorides) and bis(aryl silyl ethers) under DBU-catalysed SuFEx conditions. The multidimensional connectivity of the S(VI) hub derived from SOF₄ presents a unique opportunity for post-polymerization modification, which was demonstrated here through the controlled and near quantitative installation of aryl silyl ethers and amines to the spine of the polymer. Further derivatization of the alkyne-decorated SuFEx polymer **7** was demonstrated using CuAAC click chemistry, delivering one new AZT functionalized polymer **9** as an example of potential application in polymer–drug conjugates. The triphenylvinyl phenoxy-branched polymer **5** showed an AIE effect, while the polymer with pendant ferrocenes **15** may exhibit interesting potential properties[47]. Collectively, these examples showcase the potential of SOF₄-derived materials in diverse applications. Detailed structure studies combining AFM, high-resolution SEM, high-resolution TEM and molecular modelling reveal helical polymer structures that correlate well with the NMR data of the polymers. Although the mechanism of forming these unique polymers is not yet understood, the helical structures suggest an unprecedented degree of self-referential control, stereochemical and otherwise, over the constitution of the evolving polymer chains.

## Online content
Any methods, additional references, Nature Research reporting summaries, source data, extended data, supplementary information,

acknowledgements, peer review information; details of author contributions and competing interests; and statements of data and code availability are available at https://doi.org/10.1038/s41557-021-00726-x.

## References
1. Sharpless, K. B. & Kolb, H. C. in *Book of Abstracts*, *217th ACS National Meeting, Anaheim, CA, March 21–25* 145538 (ACS, 1999).
2. Kolb, H. C., Finn, M. G. & Sharpless, K. B. Click chemistry: diverse chemical function from a few good reactions. *Angew. Chem. Int. Ed.* **40**, 2004–2021 (2001).
3. Tornoe, C. W., Christensen, C. & Meldal, M. Peptidotriazoles on solid phase: 1,2,3-triazoles by regiospecific copper(I)-catalyzed 1,3-dipolar cycloadditions of terminal alkynes to azides. *J. Org. Chem.* **67**, 3057–3064 (2002).
4. Rostovtsev, V. V., Green, L. G., Fokin, V. V. & Sharpless, K. B. A stepwise Huisgen cycloaddition process: copper(I)-catalyzed regioselective 'ligation' of azides and terminal alkynes. *Angew. Chem. Int. Ed.* **41**, 2596–2599 (2002).
5. Dong, J., Krasnova, L., Finn, M. G. & Sharpless, K. B. Sulfur(VI) fluoride exchange (SuFEx): another good reaction for click chemistry. *Angew. Chem. Int. Ed.* **53**, 9430–9448 (2014).
6. Kolb, H. C. & Sharpless, K. B. The growing impact of click chemistry on drug discovery. *Drug Discov. Today* **8**, 1128–1137 (2003).
7. Moses, J. E. & Moorhouse, A. D. The growing applications of click chemistry. *Chem. Soc. Rev.* **36**, 1249–1262 (2007).
8. Moorhouse, A. D. & Moses, J. E. Click chemistry and medicinal chemistry: a case of 'cyclo-addiction'. *ChemMedChem* **3**, 715–723 (2008).

9. Thirumurugan, P., Matosiuk, D. & Jozwiak, K. Click chemistry for drug development and diverse chemical–biology applications. *Chem. Rev.* **113**, 4905–4979 (2013).

10. Rouhanifard, S. H., Nordstrom, L. U., Zheng, T. & Wu, P. Chemical probing of glycans in cells and organisms. *Chem. Soc. Rev.* **42**, 4284–4296 (2013).

11. McKay, C. S. & Finn, M. G. Click chemistry in complex mixtures: bioorthogonal bioconjugation. *Chem. Biol.* **21**, 1075–1101 (2014).

12. Xi, W., Scott, T. F., Kloxin, C. J. & Bowman, C. N. Click chemistry in materials science. *Adv. Funct. Mater.* **24**, 2572–2590 (2014).

13. Liu, Y. et al. Click chemistry in materials synthesis. III. Metal-adhesive polymers from Cu(I)-catalyzed azide–alkyne cycloaddition. *J. Polym. Sci. A* **45**, 5182–5189 (2007).

14. Diaz, D. D. et al. Click chemistry in materials synthesis. 1. Adhesive polymers from copper-catalyzed azide–alkyne cycloaddition. *J. Polym. Sci. A* **42**, 4392–4403 (2004).

15. Wu, P. et al. Efficiency and fidelity in a click-chemistry route to triazole dendrimers by the copper(I)-catalyzed ligation of azides and alkynes. *Angew. Chem. Int. Ed.* **43**, 3928–3932 (2004).

16. van Steenis, D. J. V. C., David, O. R. P., van Strijdonck, G. P. F., van Maarseveen, J. H. & Reek, J. N. H. Click-chemistry as an efficient synthetic tool for the preparation of novel conjugated polymers. *Chem. Commun.* **2005**, 4333–4335 (2005).

17. Srinivasachari, S., Liu, Y., Zhang, G., Prevette, L. & Reineke, T. M. Trehalose click polymers inhibit nanoparticle aggregation and promote pDNA delivery in serum. *J. Am. Chem. Soc.* **128**, 8176–8184 (2006).

18. Gahtory, D. et al. Quantitative and orthogonal formation and reactivity of SuFEx platforms. *Chem. Eur. J.* **24**, 10550–10556 (2018).

19. Randall, J. D. et al. Modification of carbon fibre surfaces by sulfur–fluoride exchange click chemistry. *ChemPhysChem* **19**, 3176–3181 (2018).

20. Kassick, A. J. et al. SuFEx-based strategies for the preparation of functional particles and cation exchange resins. *Chem. Commun.* **55**, 3891–3894 (2019).

21. Fan, H. et al. Sulfur(VI) fluoride exchange polymerization for large conjugate chromophores and functional main-chain polysulfates with nonvolatile memory performance. *ChemPlusChem* **83**, 407–413 (2018).

22. Park, S. et al. SuFEx in metal–organic frameworks: versatile postsynthetic modification tool. *ACS Appl. Mater. Interfaces* **10**, 33785–33789 (2018).

23. Li, S., Wu, P., Moses, J. E. & Sharpless, K. B. Multidimensional SuFEx click chemistry: sequential sulfur(VI) fluoride exchange connections of diverse modules launched from an SOF₄ hub. *Angew. Chem. Int. Ed.* **56**, 2903–2908 (2017).

24. Gao, B., Li, S., Wu, P., Moses, J. E. & Sharpless, K. B. SuFEx chemistry of thionyl tetrafluoride (SOF₄) with organolithium nucleophiles: synthesis of sulfonimidoyl fluorides, sulfoximines, sulfonimidamides and sulfonimidates. *Angew. Chem. Int. Ed.* **57**, 1939–1943 (2018).

25. Zheng, Q., Dong, J. & Sharpless, K. B. Ethenesulfonyl fluoride (ESF): an on-water procedure for the kilogram-scale preparation. *J. Org. Chem.* **81**, 11360–11362 (2016).

26. Smedley, C. J. et al. 1-Bromoethene-1-sulfonyl fluoride (BESF) is another good connective hub for SuFEx click chemistry. *Chem. Commun.* **54**, 6020–6023 (2018).

27. Leng, J. & Qin, H.-L. 1-Bromoethene-1-sulfonyl fluoride (1-Br-ESF), a new SuFEx clickable reagent, and its application for regioselective construction of 5-sulfonylfluoro isoxazoles. *Chem. Commun.* **54**, 4477–4480 (2018).

28. Thomas, J. & Fokin, V. V. Regioselective synthesis of fluorosulfonyl 1,2,3-triazoles from bromovinylsulfonyl fluoride. *Org. Lett.* **20**, 3749–3752 (2018).

29. Dong, J., Sharpless, K. B., Kwisnek, L., Oakdale, J. S. & Fokin, V. V. SuFEx-based synthesis of polysulfates. *Angew. Chem. Int. Ed.* **53**, 9466–9470 (2014).

30. Gao, B. et al. Bifluoride-catalysed sulfur(VI) fluoride exchange reaction for the synthesis of polysulfates and polysulfonates. *Nat. Chem.* **9**, 1083–1088 (2017).

31. Wang, H. et al. SuFEx-based polysulfonate formation from ethenesulfonyl fluoride-amine adducts. *Angew. Chem. Int. Ed.* **56**, 11203–11208 (2017).

32. Cowie, J. M. G. & Arrighi, V. in *Polymers*: *Chemistry and Physics of Modern Materials* 3rd edn (eds Cowie, J. M. G. & Arrighi, V.) 29–56 (CRC Press, 2007).

33. Gauthier, M. A., Gibson, M. I. & Klok, H.-A. Synthesis of functional polymers by post-polymerization modification. *Angew. Chem. Int. Ed.* **48**, 48–58 (2009).

34. Boaen, N. K. & Hillmyer, M. A. Post-polymerization functionalization of polyolefins. *Chem. Soc. Rev.* **34**, 267–275 (2005).

35. Yatvin, J., Brooks, K. & Locklin, J. SuFEx on the surface: a flexible platform for postpolymerization modification of polymer brushes. *Angew. Chem. Int. Ed.* **54**, 13370–13373 (2015).

36. Oakdale, J. S., Kwisnek, L. & Fokin, V. V. Selective and orthogonal post-polymerization modification using sulfur(VI) fluoride exchange (SuFEx) and copper-catalyzed azide–alkyne cycloaddition (CuAAC) reactions. *Macromolecules* **49**, 4473–4479 (2016).

37. Brooks, K. et al. SuFEx postpolymerization modification kinetics and reactivity in polymer brushes. *Macromolecules* **51**, 297–305 (2018).

38. Hong, Y., Lam, J. W. Y. & Tang, B. Z. Aggregation-induced emission. *Chem. Soc. Rev.* **40**, 5361–5388 (2011).

39. del Amo, D. S. et al. Biocompatible copper(I) catalysts for in vivo imaging of glycans. *J. Am. Chem. Soc.* **132**, 16893–16899 (2010).

40. Wang, W. et al. Sulfated ligands for the copper(I)-catalyzed azide–alkyne cycloaddition. *Chem. Asian J.* **6**, 2796–2802 (2011).

41. Yashima, E., Maeda, K., Iida, H., Furusho, Y. & Nagai, K. Helical polymers: synthesis, structures and functions. *Chem. Rev.* **109**, 6102–6211 (2009).

42. Nakano, T. & Okamoto, Y. Synthetic helical polymers: conformation and function. *Chem. Rev.* **101**, 4013–4038 (2001).

43. BIOVIA, Materials Studio 6.0 (Dassault Systems).

44. Li, Y. et al. Hybrids of organic molecules and flat, oxide-free silicon: high-density monolayers, electronic properties and functionalization. *Langmuir* **28**, 9920–9929 (2012).

45. Bose, K., Lech, C. J., Heddi, B. & Anh Tuan, P. High-resolution AFM structure of DNA G-wires in aqueous solution. *Nat. Commun.* **9**, 1959 (2018).

46. Liang, D.-D. et al. Silicon-free SuFEx reactions of sulfonimidoyl fluorides: scope, enantioselectivity and mechanism. *Angew. Chem. Int. Ed.* **59**, 7494–7500 (2020).

47. Pietschnig, R. Polymers with pendant ferrocenes. *Chem. Soc. Rev.* **45**, 5216–5231 (2016).

## Methods

Full details of the methods are provided in the Supplementary Information.

**General information.** $^1$H spectra were recorded on Bruker AV-600 and Bruker AV-400 NMR instruments. $^{13}$C NMR spectra were recorded on a Bruker AV-600 instrument. $^{19}$F NMR spectra were recorded on a Bruker AV-400 instrument. The chemical shifts ($\delta$) are expressed in parts per million relative to trimethylsilyl or residual deuterated acetonitrile (CH$_3$CN), with DMF and DMSO as internal standards. $^1$H NMR spectra were recorded at 600 or 400 MHz. $^{13}$C NMR spectra were recorded at 151 MHz or 101 MHz. $^{19}$F NMR spectra were recorded at 376 MHz. NMR acquisitions were performed at 295 K unless otherwise noted. Abbreviations are s, singlet; d, doublet; t, triplet; q, quartet; p, pentet; br s, broad singlet. Infrared spectra were recorded as pure, undiluted samples using a ThermoNicolet Avatar 370 Fourier transform infrared spectrometer with a Smart MIRacle HATR attachment. Melting points (mp) were determined using a Thomas–Hoover melting point apparatus and are uncorrected. GC-MS data were recorded on an Agilent 7890A GC system with an Agilent 5975C Inert MSD system or Shimadzu GC-MS-QP2010 SE operating in electron impact (EI+) mode. LC-MS was performed on an Agilent 1260 LC/MSD instrument with an Agilent 6120 quadrupole mass spectrometer (electrospray ionization, ES) or a Waters ACQUITY ARC-ACQUITY QDa eluting with 0.1% trifluoroacetic acid in H$_2$O and 0.05% trifluoroacetic acid in CH$_3$CN. Waters UPLC (Acquity Arc) and Waters preparative HPLC (2545) systems were used for e.e. analysis and chiral sample preparation. High-resolution mass spectrometry was performed on an Agilent ES-TOF instrument. Single-crystal X-ray diffraction was carried out on an Agilent SuperNova single-crystal diffractometer. Precoated Merck F-254 silica gel plates were used for thin-layer analytical chromatography (TLC) and visualized with short-wave UV light or by potassium permanganate stain. Column chromatography was performed using EMD (Merck) silica gel 60 (40–63 µm). Extra dry solvents over molecular sieves were purchased from Aldrich or Acros Organics, including CH$_3$CN, THF, DMF and NMP. All of the bis(amines) used in this study are available commercially.

The polymer weight-averaged molecular weight ($M_w^{ps}$) and PDI relative to polystyrene were measured using a Waters 1515 gel permeation chromatography (GPC) system. This was equipped with a diode array, a refractive index detector 2414 and a series of MZ-Gel SDplus 500 Å, 10$^3$ Å and 10$^4$ Å columns. The system was calibrated with EasyVial PS-M polystyrene standards (Agilent Technologies, $M_p$ = 364,000, 217,900, 113,300, 47,190, 30,230, 13,270, 6,940, 2,780, 1,220, 935, 370 and 162 g mol$^{-1}$). HPLC-grade DMF was used as a mobile phase with 0.05 mol l$^{-1}$ of LiBr as additive (Acros Organics, 99.999% grade). The elution rate was 0.8 ml min$^{-1}$ (column temperature, 40 °C). All samples/standards were tested at loadings of 100 µl (1.0 mg ml$^{-1}$).

Thermal gravimetric analysis (TGA) and differential scanning calorimetry (DSC) analysis were carried out at Lawrence Berkeley National Laboratory and Soochow University. TGA was carried out on a TGA-MS Q5000 system under nitrogen using aluminium pans (20 °C min$^{-1}$, starting from 25 °C and ending at 600 °C). DSC was carried out on a TA Q200 instrument with a heat rate of 5 °C min$^{-1}$.

*Procedure for the synthesis of polymer 3-1 on a 30 mmol scale.* To a round-bottomed flask (250 ml) with a magnetic stir bar was added the bis(iminosulfur oxydifluoride) **1-1** (12.5 g, 30.0 mmol), BPA-TBS **2-1** (13.7 g, 30.0 mmol) and 40 ml of anhydrous NMP. The flask was sealed with a Suba-Seal Septa, vacuumized with a needle linked to a pump, until no bubbles formed in the solution (5–10 min). DBU (91.3 mg, 90 µl, 0.60 mmol, $d$ = 1.018 g ml$^{-1}$) was added into the flask via a needle. After stirring at room temperature for 15 min, the solution became a jam, and the stir bar stopped moving. After staying at room temperature for 3.5 h, 50 ml of DMF was added. The flask was shaken to promote dissolution, and the resulting solution was poured slowly into 600 ml of MeOH with mechanical stirring. The solution was stirred in MeOH for 20 min and filtrated. The white solid was washed with MeOH three times (150 ml × 3) and dried in a vacuum oven (60 °C) for 24 h to give 18.0 g of polymer **3-1** (99%). $M_w^{ps}$ = 197 kDa, PDI = 1.8, $T_g$ (glass transition temperature, DSC) = 150.8 °C, $T_d$ (decomposition temperature, 5% weight loss, TGA) = 261.2 °C. $^1$H NMR (600 MHz, DMF-$d_7$) δ 8.05 (d, $J$ = 8.4 Hz, 4H), 7.58–7.36 (m, 12H), 1.70 (s, 6H). $^{13}$C NMR (151 MHz, DMF-$d_7$) δ 151.90, 149.29, 144.39 (d, $J$ = 2.7 Hz), 139.14, 130.56, 130.11, 125.68 (d, $J$ = 2.8 Hz), 122.26, 43.87, 31.09. $^{19}$F NMR (376 MHz, DMF-$d_7$) δ 50.69.

**AFM, SEM and TEM experiments.** *AFM.* Surface preparation. A Si(111) wafer with a 0.2° miscut angle along ⟨112⟩ was first cut (10 × 10 mm$^2$) and subsequently cleaned in a sonication bath with acetone, ethanol and then with Milli-Q water (resistivity of >18 MΩ cm). The Si wafer was oxidized in oxygen plasma for at least 20 min, after which the substrates were immersed immediately in water and rinsed thoroughly, followed by drying with a stream of argon. Subsequently, the substrates were etched in an argon-saturated 40% aqueous NH$_4$F solution for 15 min, rinsed by Milli-Q water and finally dried with a stream of argon. After being etched, the samples were rinsed with argon-saturated water and finally blown dry with a stream of argon. These samples were then immediately transferred to an inert-atmosphere glove box. Next, the surface was placed into a neat dry and

pure 1-hexadecyne solution, which was then heated. The reactions were performed at 80 °C overnight (typically 16 h). Afterwards, the mixture was allowed to cool to room temperature, the coated surface was taken out of the solution, taken out of the glove box, and immediately extensively rinsed with pentane and CH$_2$Cl$_2$. The sample was sonicated for 5 min in CH$_2$Cl$_2$ to remove physisorbed molecules, after which the samples were blown dry with a stream of dry argon. Before depositing the polymer solution onto such a hexadecyne-modified Si(111) surface, AFM was used to check that it was atomically flat (root-mean-square roughness of <0.1 nm). To determine the helicity of the polymer, the AFM morphology and amplitude maps were first flattened in series by a first-order plane fit and by a second-order polynomial line-by-line fit. Subsequently, a 7 × 7 weak median filter was applied to reduce the level of noise. FFT was calculated on the raw cross-sectional profiles after a zero-order profile subtraction. Analysis was performed with SPIP 8.3 software (Image Metrology).

Polymer deposition. Two drops (~10 µl) of a polymer solution (for example of **3-23**, 0.1 mg ml$^{-1}$ in HPLC-grade DCM) were gently dropped on such a hexadecyne-coated surface, after which the solvent smoothly evaporated at room temperature without enforcing. The imaging was performed in tapping mode in air using either OMCL-AC240 silicon cantilevers (Olympus Corporation) with a stiffness of 1.54 N m$^{-1}$ or ultra-sharp silicon tips from NanoAndMore SHR75, with a stiffness of 3 N m$^{-1}$ and radius <1 nm. Images were flattened with a third-order flattening procedure using the MFP-3D software. Topographies were typically obtained on two different instruments (Asylum MFP-3D AFM and JEOL JSPM-5400 scanning probe microscopes) and displayed near-identical features on both.

*SEM and AES.* AES measurements were performed at room temperature with a scanning Auger electron spectroscopy (JEOL JAMP-9500F field emission scanning Auger microprobe) system. Samples were prepared by spreading powder particles over a gold-coated surface. AES spectra were acquired with a primary beam of 2 keV. For Auger elemental analysis, an 8-nm probe diameter was used. Elemental mapping was analysed by AES. Elemental images were acquired with a primary beam of 2 keV. The take-off angle of the instrument was 0°.

*TEM and SEM.* For the polymer solutions (0.2 mg ml$^{-1}$ in THF), an ultrathin carbon grid (thickness of ~4 nm, Ted Pella ultrathin carbon film on lacey carbon support film, 400 mesh, copper) was pretreated by a plasma cleaner for 10 s, then a drop of the diluted sample in THF was deposited on the grid surface for a few seconds, and the excess of solution was removed by fibre-free paper. This grid was dipped in uranyl acetate solution, then the excess of uranyl solution was removed by fibre-free paper. In this study, uranyl acetate was used as a negative stain for imaging. For TEM analysis, the TEM grid was mounted in a single tilt sample holder and then introduced into the microscope for imaging. TEM analyses were performed using a Titan FEG-300KV system, a 4k Ceta camera and GMS software for data acquisition. For scanning electron microscopy (SEM) measurements, the same TEM grid was mounted in the SEM, an FEI field emission Quanta FEG450 SEM using a solid-state back scattering electron detector (VCD).

*Molecular mechanics studies.* Geometry optimization of the polymers was performed using molecular mechanics calculations with the PCFF as implemented in the Dassault BIOVIA, Materials Studio 6.0, San Diego molecular modelling package. To this aim, the polymer structure was first drawn in ChemDraw with 32 repeating units. This structure was transferred into Chem3D, optimized using the MMFF94 force field as implemented in that, and the resulting structure saved and converted to the *.mol format, which can be read by Materials Studio. This structure was then imported in Materials Studio and further optimized using the Forcite minimizer and the PCFF force field, with 'high-convergence' criteria and the 'smart optimizer' algorithm. No further restrictions were applied.

## Data availability

Data supporting the findings of this study are available within the Article and its Supplementary Information. Crystallographic data for the structures reported in this Article have been deposited at the Cambridge Crystallographic Data Centre, under deposition no. CCDC 2026570 [(**R**)-(−)-**16**]. Copies of the data can be obtained free of charge via https://www.ccdc.cam.ac.uk/structures/. Source data are provided with this paper.

## Acknowledgements

## Author contributions

K.B.S., J.M. and H.Z. supervised the work. S.L., K.B.S., P.W., J.L. and J.M. conceived and designed the syntheses of the SOF$_4$-derived polymers. S.L., G.L., B.G., S.P.P., X.C. and H.K. performed the synthesis and characterization of the polymers. F.Z., L.M.K., Y.L. and J.L. collected and analysed the DSC and TGA data for all polymers. F.Z. collected the XRD data. S.P.P. performed molecular modelling, AFM and scanning Auger experiments. H.D. performed the SEM and TEM experiments. D.-D.L. collected the circular dichroism data. S.L., H.Z., K.B.S. and J.M. contributed to the preparation of the manuscript. All authors discussed the results and commented on the manuscript.

## Competing interests

K.B.S., P.W., S.L. and B.G. are named as inventors on a patent applicant filed by The Scripps Research Institute (provisional patent application US62/427,489, filed on 29 November 2016, and international patent application no. PCT/US2017/063746).

## Additional information

**Supplementary information** The online version contains supplementary material available at https://doi.org/10.1038/s41557-021-00726-x.

**Correspondence and requests for materials** should be addressed to S.L., P.W., H.Z., J.M. or K.B.S.

**Peer review information** *Nature Chemistry* thanks Jason Locklin, Jia Niu and the other, anonymous, reviewer(s) for their contribution to the peer review of this work.

**Reprints and permissions information** is available at www.nature.com/reprints.